# New rare earth hafnium oxynitride perovskites with photocatalytic activity in water oxidation and reduction

Ashley P. Black, Hajime Suzuki, Masanobu Higashi, Carlos Frontera, Clemens Ritter, Chandan De, A.Sundaresan, Ryu Abe and Amparo Fuertes

## Supplementary Information

Experimental Details

The oxynitrides $LnHfO_2N$( Ln= La, Nd, Sm) were prepared by solid state reaction in $N_2$ (Air Liquide, 99.9999 %) of stoichiometric mixtures of $Hf_2ON_2$ and $La_2O_3$ (Aldrich, 99.99 %), $Nd_2O_3$ (Aldrich, 99.9 %) or $Sm_2O_3$ (Alfa Aesar, 99.998 %). $Hf_2ON_2$ was prepared by treatment of $HfO_2$ (Alfa Aesar, 99.95 %) under $NH_3$ flow of 600 $cm^3$/min (Carburos Metálicos, 99.9%) during 35 hours at 980$^o$C with three intermediate regrindings. $La_2O_3$, $Nd_2O_3$ and $Sm_2O_3$ were previously treated during 12 hours under Ar at 900 $^o$C. Handling of the reactants was carried out in a glove box under recirculating argon atmosphere. The powders were thoroughly mixed in an agate mortar for 30 min, pressed into a pellet, placed in a molybdenum crucible and covered with a zirconium foil as oxygen/water scavenger. The mixtures were treated at 1500 °C during 3 hours with heating and cooling rates of 300 °C/h.

$LaZrO_2N$ was synthesised by a solid state reaction in $N_2$ of the stoichiometric mixture of ZrN (Alfa Aesar, 99.5 %), $ZrO_2$ (Aldrich, 99.99 %), and $La_2O_3$. $ZrO_2$ was previously treated during 12 hours under Ar at 600$^o$C and ZrN was dried during 12 hours at 75 $^o$C under a dynamic vacuum. $La_2O_3$ was previously treated during 12 hours under Ar at 900 $^o$C. The powders were thoroughly mixed in an agate mortar for 30 min in the glove box, pressed into a pellet, placed in a molybdenum crucible and covered with a zirconium foil. The pellet was first treated at 600 $^o$C during 3 hours followed by treatment at 1500 $^o$C for 25 hours using heating and cooling rates of 300 °C/h. The obtained sample contained small amounts of $La_2Zr_2O_7$ and ZrN.

EDS analyses were performed in a FEI Quanta 200 FEG scanning electron microscope equipped with a EDAX detector with an energy resolution of 132 eV. N contents were determined by combustion analysis in oxygen in a Thermo Fisher Scientific instrument, heating the samples in oxygen up to 1060 $^o$C and using MgO, $WO_3$ and Sn as additives and atropine as a reference standard. Thermogravimetric analysis in oxygen was performed in a NETZSCH-STA 449 F1 Jupiter. The samples were heated at 10 $^o$C/min to 1000 $^o$C under $O_2$ at a flow rate of 70 $cm^3$/min.

X-ray powder diffraction data were collected on a Siemens D5000 diffractometer using Cu Kα radiation (λ= 1.5418 Å). Synchrotron X-ray powder diffraction data at room temperature were measured from capillary (0.3 mm diameter) samples in the angular range $1.038^o \leq 2\theta \leq 61.09^o$ at the MSPD beamline [1] of the ALBA Synchrotron (Cerdanyola del Vallès, Spain). Using a double Si (111) crystal monochromator, a short wavelength was selected and calibrated with Si NIST ($\lambda$ = 0.619604 Å). Rietveld analysis was carried out using the program Fullprof.[2] Background refinement was performed by linear interpolation and the data were corrected for absorption.

Neutron powder diffraction data for $LaHfO_2N$ and $NdHfO_2N$ were recorded at room temperature using 0.1 g samples on the D20 diffractometer at the Institut Laue-Langevin (ILL), Grenoble, France. The neutron wavelength was 1.5423 Å using the 90° take-off angle. Neutron powder diffraction data for $LaZrO_2N$ were recorded on the HRPD diffractometer at the ISIS spallation source, Rutherford Appleton Laboratory, U.K. The structural model was refined

against data collected from the 90° detector bank, which provides a d-spacing range of 0.6 – 2.5 Å. Rietveld analysis was carried out using the program Fullprof.

Diffuse reflectance spectra were registered at room temperature on a UV-Vis-NIR Varian Cary 5000 spectrophotometer, with operational range of 190-3300 nm.

X-ray photoelectron spectroscopy (XPS) of the catalysts was performed using an ULVAC-PHI 5500MT system. The spectra were measured at room temperature using Mg Kα radiation. The XPS binding energies for each sample were corrected with reference to the C 1s peak of the carbon impurity (284.8 eV).

Electrical measurements were performed in Physical Property Measurement System (PPMS, Quantum Design, USA) using a custom made multifunctional probe. DC resistivity was measured using a Keithley Electrometer/High resistance meter (model 6517A). Dielectric properties were measured using the Agilent (E4980A) Precision LCR meter. Electrical contacts to the sample were made using silver paste and copper wire. The data were recorded while warming the sample.

Photocatalytic reactions were carried out in a Pyrex reaction vessel connected to a closed gas circulation system. For the hydrogen evolution test in the presence of an electron donor, Pt-loaded $LnHfO_2N$ (Ln=La,Nd,Sm) or $LaZrO_2N$ (50 mg) was suspended in 250 ml of an aqueous MeOH solution (20 % vol) and for the oxygen evolution test 50 mg of $LnHfO_2N$ (Ln=La,Nd,Sm) or $LaZrO_2N$ were suspended in 250 ml of an aqueous $AgNO_3$ solution (10 mM). The reactant solutions were evacuated several times to completely remove any air prior to irradiation under a 300 W xenon lamp. For visible light irradiation, a cutoff filter (L42) was fitted to the aforementioned light source ($420 < \lambda < 800$ nm). The reactant solution was maintained at room temperature by a flow of cooling water during the reaction. The evolved gases were analyzed by gas chromatography. Platinum (0.3 wt%) or (1 wt%) co-catalyst was deposited by an impregnation method. Typically, 55 mg of $LnHfO_2N$ (Ln=La,Nd,Sm) or $LaZrO_2N$ were dispersed in 150 µl of a $H_2PtCl_6$ solution. After sonication during 3 min, the slurry was dried on a water bath and finally treated at 200 $^oC$ under $H_2$ flow (20 ml/min) for 0.5 h. Water oxidation tests were performed on bare $LnHfO_2N$ (Ln=La, Nd) and on $IrO_x$(1wt%, calculated as metal)-$LnHfO_2N$ samples for Ln= La and Sm. Iridium oxide was loaded by an impregnation method from $Na_2IrCl_6$ aqueous solution, followed by oxidation in air at 573 K for 0.5 h. For the zirconium sample, cobalt oxide was used as $O_2$ evolution co-catalyst. (3 wt%, calculated as metal) $CoO_x$ was deposited from a $Co(NO_3)_2$ aqueous solution by an impregnation method and dried in air at room temperature.

**Table S1. Summary of the *Pnma* model for $LaHfO_2N$ refined against room temperature synchrotron X-ray powder diffraction data.**

| Cell parameters (Å) | | | | Agreement factors | |
|---|---|---|---|---|---|
| a = 5.83312(1) | | | | $R_{Bragg}$ = 1.35 % | |
| b = 8.20182(2) | | | | $R_{wp}$ = 2.76 % | |
| c = 5.79828(1) | | | | $\chi^2$ = 3.44 | |
| Atom | Site | x | y | z | $B_{iso}$ (Å$^2$) |
| La | 4c | 0.02922(6) | 0.25 | 0.99255(17) | 1.302(1) |
| Hf | 4b | 0.5 | 0 | 0 | 0.9324(8) |
| X1 | 4c | 0.4757(9) | 0.25 | 0.0889(12) | 0.52(2) |
| X2 | 8d | 0.2958(8) | 0.0480(7) | 0.7128(11) | 1.24(2) |
| | | La-X1 | La-X2 | Hf-X1 | Hf-X2 |
| Bond length / Å | | 3.277(5) | 2.792(6) ×2 | 2.119(2)×2 | 2.085(6)×2 |
| | | 2.664(5) | 2.453(6)×2 | | 2.157(5)×2 |
| | | 3.386(7) | 3.534(6)×2 | | |
| | | 2.447(7) | 2.940(6)×2 | | |
| $\langle La-O/N \rangle$ | | 2.934(2) | | $\langle Hf-O/N \rangle$ | 2.120 (2) |

**Table S2. Summary of the *Pnma* model for $NdHfO_2N$ refined against room temperature synchrotron X-ray powder diffraction data.**

| Cell parameters (Å) | | | | Agreement factors | |
|---|---|---|---|---|---|
| a = 5.82227(2) | | | | $R_{Bragg}$ = 2.24 % | |
| b = 8.13418(2) | | | | $R_{wp}$ = 4.82 % | |
| c = 5.69967(1) | | | | $\chi^2$ = 4.50 | |
| Atom | Site | x | y | z | $B_{iso}$ (Å$^2$) |
| Nd | 4c | 0.04316(8) | 0.25 | 0.98835(20) | 1.048(2) |
| Hf | 4b | 0.5 | 0 | 0 | 0.747(1) |
| X1 | 4c | 0.4615(14) | 0.25 | 0.0980(14) | 1.13(3) |
| X2 | 8d | 0.2961(10) | 0.0575(8) | 0.7023(11) | 0.81(2) |
| | | Nd-X1 | Nd-X2 | Hf-X1 | Hf-X2 |
| Bond length / Å | | 3.444(8) | 2.698(6)×2 | 2.121(2)×2 | 2.123(6)×2 |
| | | 2.515(8) | 2.388(6)×2 | | 2.126(6)×2 |
| | | 3.376(8) | 3.642(6)×2 | | |
| | | 2.405(8) | 2.936(6)×2 | | |
| $\langle Nd-O/N \rangle$ | | 2.922(2) | | $\langle Hf-O/N \rangle$ | 2.123(2) |

**Table S3. Summary of the *Pnma* model for $SmHfO_2N$ refined against room temperature synchrotron X-ray powder diffraction data.**

| Cell parameters (Å) | | | | Agreement factors | |
|---|---|---|---|---|---|
| a = 5.81768(2) | | | | $R_{Bragg}$ = 4.13 % | |
| b = 8.09702(3) | | | | $R_{wp}$ = 10.6 % | |
| c = 5.65555(2) | | | | $\chi^2$ = 3.40 | |
| Atom | Site | x | y | z | $B_{iso}$ (Å$^2$) |
| Sm | 4c | 0.04798(11) | 0.25 | 0.9880(3) | 0.81(2) |
| Hf | 4b | 0.5 | 0 | 0 | 0.49(1) |
| X1 | 4c | 0.4478(18) | 0.25 | 0.105(2) | 0.43(4) |
| X2 | 8d | 0.2933(16) | 0.0590(12) | 0.6890(16) | 1.01(4) |
| | | Sm-X1 | Sm-X2 | Hf-X1 | Hf-X2 |
| Bond length / Å | | 3.554(11) | 2.700(9)×2 | 2.131(3)×2 | 2.184(9)×2 |
| | | 2.418(11) | 2.364(9)×2 | | 2.069(9)×2 |
| | | 3.404(11) | 3.680(9)×2 | | |
| | | 2.374(11) | 2.899(10)×2 | | |
| $\langle Sm-O/N \rangle$ | | 2.920 (3) | | $\langle Hf-O/N \rangle$ | 2.128(3) |

**Table S4. Summary of the *Pnma* model for $NdHfO_2N$ refined against room temperature neutron powder diffraction data.**

| Cell parameters (Å) | | | | Agreement factors | | |
|---|---|---|---|---|---|---|
| a = 5.8284(1) | | | | $R_{Bragg}$ = 4.45 % | | |
| b = 8.1383(2) | | | | $R_{wp}$ = 2.93 % | | |
| c = 5.7012 (1) | | | | $\chi^2$ = 3.92 | | |
| Atom | Site | x | y | z | $B_{iso}$ (Å$^2$) | (O/N) Occ. |
| Nd | 4c | 0.0419( 2) | 0.25 | 0.9902(4) | 0.51(3) | |
| Hf | 4b | 0.5 | 0 | 0 | 0.37(3) | |
| X1 | 4c | 0.4652( 4) | 0.25 | 0.1020(4) | 0.91( 2) | 0.68(2)/0.32 |
| X2 | 8d | 0.2963( 2) | 0.0533(2) | 0.7019(2) | 0.83(1) | 0.66/0.34 |
| | | | Nd-X1 | Nd-X2 | Hf-X1 | Hf-X2 |
| Bond length / Å | | | 3.421(3) | 2.732(2)×2 | 2.1257(7)×2 | 2.118 (1)×2 |
| | | | 2.548(3) | 2.411(2) ×2 | | 2.120 (1)×2 |
| | | | 3.406(3) | 3.614(2) ×2 | | |
| | | | 2.368(3) | 2.905(2)×2 | | |
| $\langle Nd-O/N \rangle$ | | 2.9223(7) | | | $\langle Hf-O/N \rangle$ | 2.1213(4) |

**Table S5. Summary of the *Pnma* model for $LaZrO_2N$ refined against room temperature synchrotron X-ray powder diffraction data.**

| Cell parameters (Å) | | | | Agreement factors | |
|---|---|---|---|---|---|
| a = 5.87471(1) | | | | $R_{Bragg}$ = 4.48 % | |
| b = 8.24302(2) | | | | $R_{wp}$ = 2.19 % | |
| c = 5.81034(1) | | | | $\chi^2$ = 2.36 | |
| Atom | Site | x | y | z | $B_{iso}$ (Å$^2$) |
| La | 4c | 0.03461(11) | 0.25 | 0.9898(2) | 1.213(3) |
| Zr | 4b | 0.5 | 0 | 0 | 0.317(4) |
| X1 | 4c | 0.4699(14) | 0.25 | 0.0964(13) | 1.65(4) |
| X2 | 8d | 0.2859(11) | 0.0482(7) | 0.7083(11) | 0.94(3) |
| | | La-X1 | La-X2 | Zr-X1 | Zr-X2 |
| Bond length / Å | | 3.375(8) | 2.761(6)×2 | 2.143 (2)×2 | 2.148(6)×2 |
| | | 2.631(8) | 2.495(6)×2 | | 2.108 (6)×2 |
| | | 3.427(8) | 3.559(6)×2 | | |
| | | 2.434(8) | 2.961(6)×2 | | |
| $\langle La-O/N \rangle$ | | 2.952(2) | | $\langle Zr-O/N \rangle$ | 2.133(2) |

**Table S6. Summary of the *Pnma* model for $LaZrO_2N$ refined against room temperature neutron powder diffraction data.**

| Cell parameters (Å) | | | | Agreement factors | | |
|---|---|---|---|---|---|---|
| a = 5.8765 (8) | | | | $R_{Bragg}$ = 7.07 % | | |
| b = 8.2465 (11) | | | | $R_{wp}$ = 5.96 % | | |
| c = 5.8128 (8) | | | | $\chi^2$ = 1.62 | | |
| Atom | Site | x | y | z | $B_{iso}$ (Å$^2$) | (O/N) Occ. |
| La | 4c | 0.0337( 3) | ¼ | 0.9934(6) | 0.221(7) | |
| Zr | 4b | 0.5 | 0.0 | 0.0 | 0.056(8) | |
| X1 | 4c | 0.4727( 5) | 0.25 | 0.0916(5) | 0.53(2) | 0.64(1)/0.36 |
| X2 | 8d | 0.2918( 3) | 0.0505(2) | 0.7085(3) | 0.35(1) | 0.68/0.32 |
| | | La-X1 | La-X2 | Zr-X1 | Zr-X2 | |
| Bond length / Å | | 3.346(3) | 2.784(3)×2 | 2.1353(8)×2 | 2.131(2)×2 | |
| | | 2.642(4) | 2.471(3) ×2 | | 2.141(2)×2 | |
| | | 3.419(5) | 3.578(3) ×2 | | | |
| | | 2.439(5) | 2.959(2)×2 | | | |
| $\langle La-O/N \rangle$ | 2.955(1) | | | $\langle Zr-O/N \rangle$ | 2.1358(7) | |

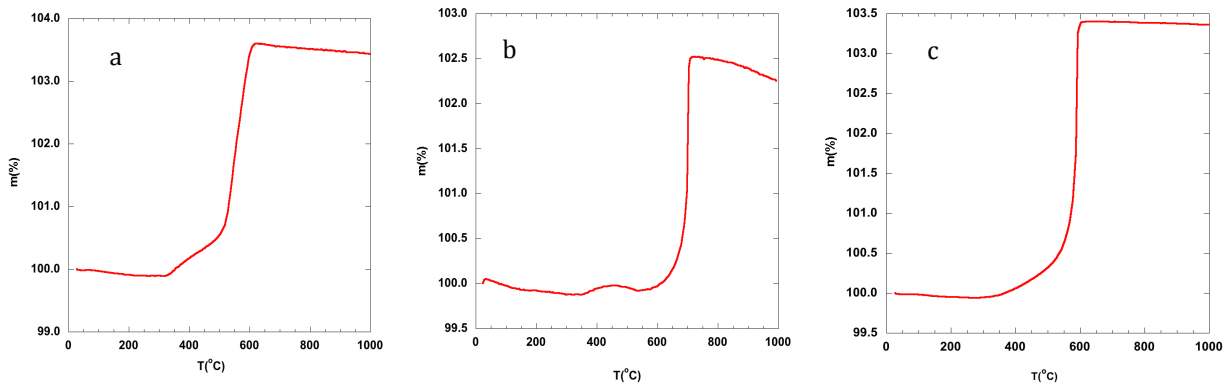


**Figure S1. Thermogravimetric analysis under oxygen gas of (a) $LaHfO_2N$, (b) $NdHfO_2N$ and (c) $SmHfO_2N$.**

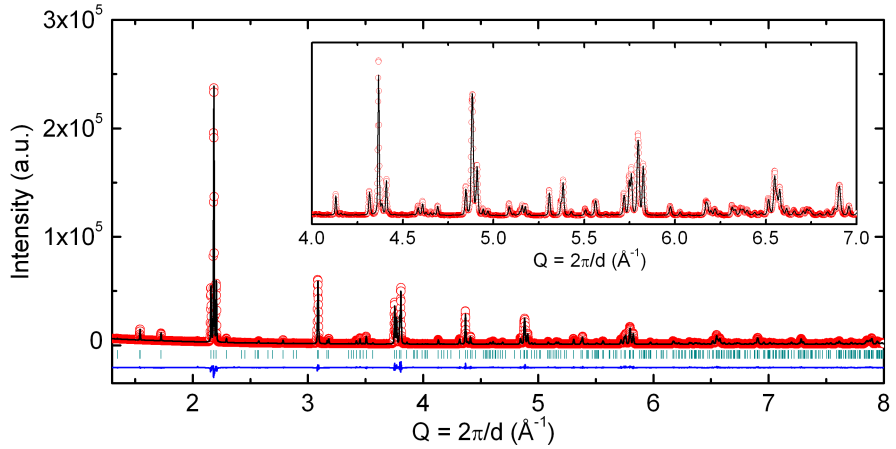


**Figure S2. Observed and calculated synchrotron X-ray powder diffraction patterns at room temperature for $NdHfO_2N$. The inset shows a magnification of the high Q region.**

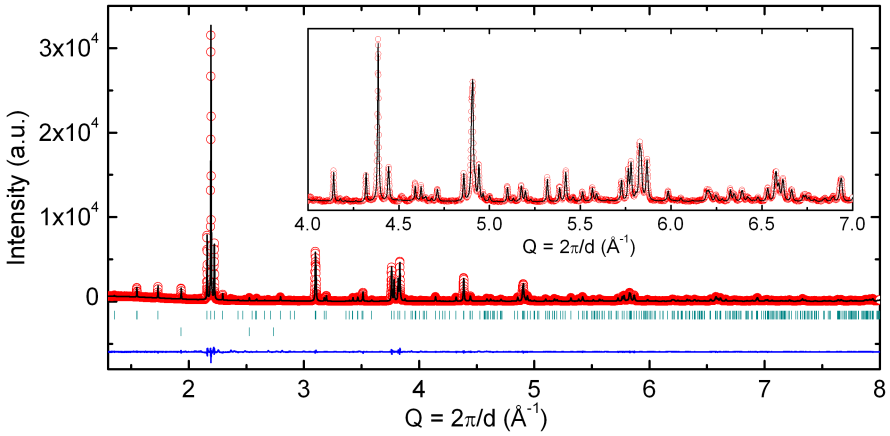


**Figure S3. Observed and calculated synchrotron X-ray powder diffraction patterns at room temperature for $SmHfO_2N$. Tick marks indicate allowed reflections for $SmHfO_2N$ (upper set) and $TiO_2$ from the cryostat (lower set). The inset shows a magnification of the high Q region.**

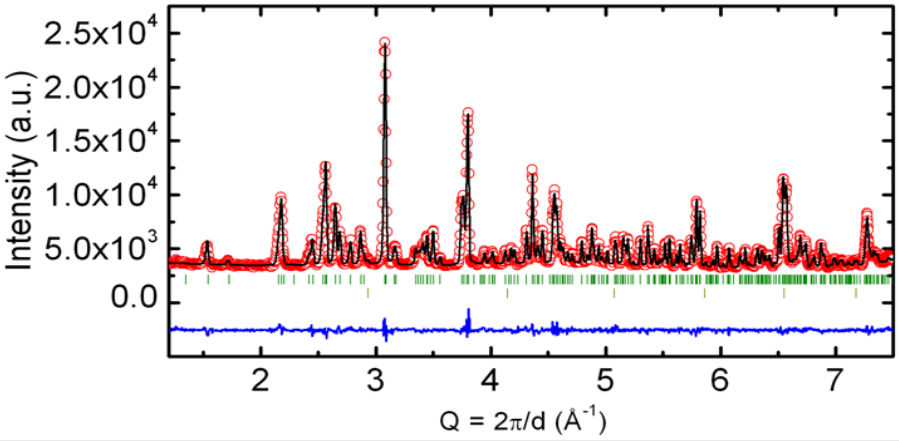


**Figure S4. Rietveld fit to room temperature neutron powder diffraction patterns for $NdHfO_2N$. Tick marks indicate allowed reflections for $NdHfO_2N$ (upper set) and V from the sample holder (lower set).**

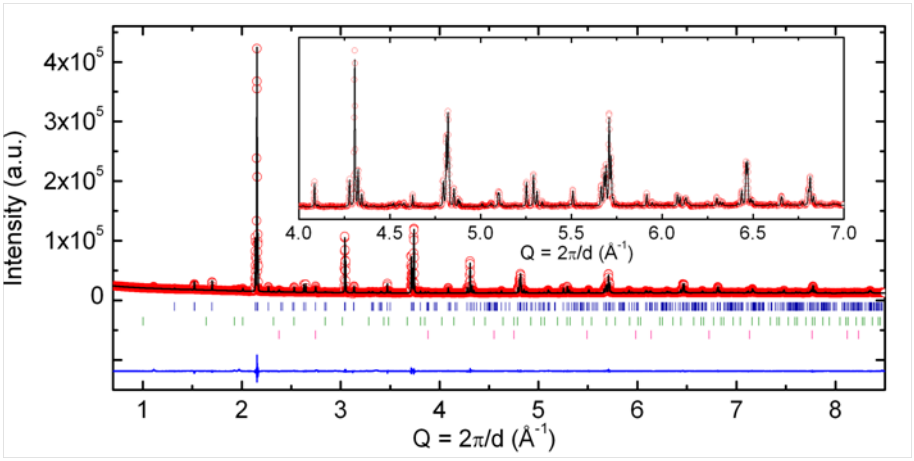


**Figure S5. Observed and calculated synchrotron X-ray powder diffraction patterns at room temperature for $LaZrO_2N$ sample. Tick marks indicate allowed reflections for $LaZrO_2N$ (upper set), $La_2Zr_2O_7$ impurity (middle set) and ZrN impurity (lower set). The inset shows a magnification of the high Q region.**

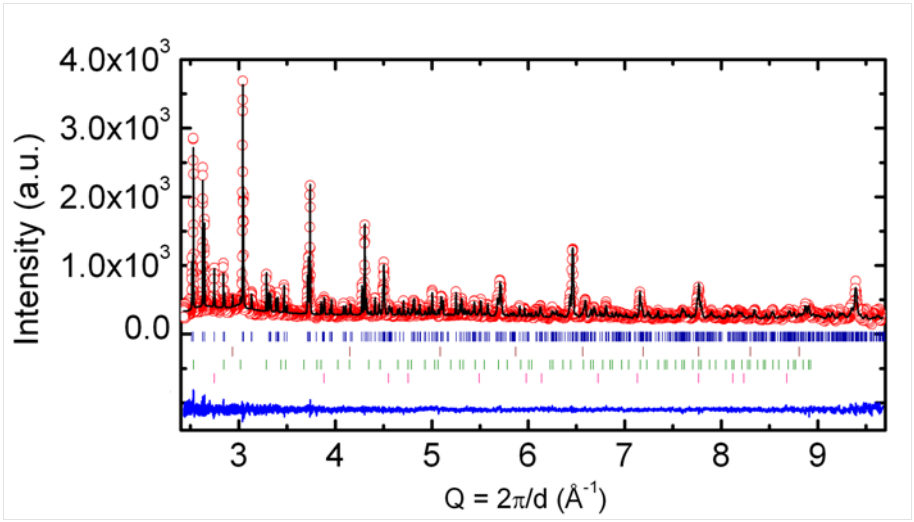


**Figure S6. Rietveld fit to room temperature neutron powder diffraction patterns for $LaZrO_2N$ sample. Tick marks indicate allowed reflections for $LaZrO_2N$ (upper set), V from the sample holder (middle upper set), $La_2Zr_2O_7$ (middle lower set) and ZrN (lower set).**

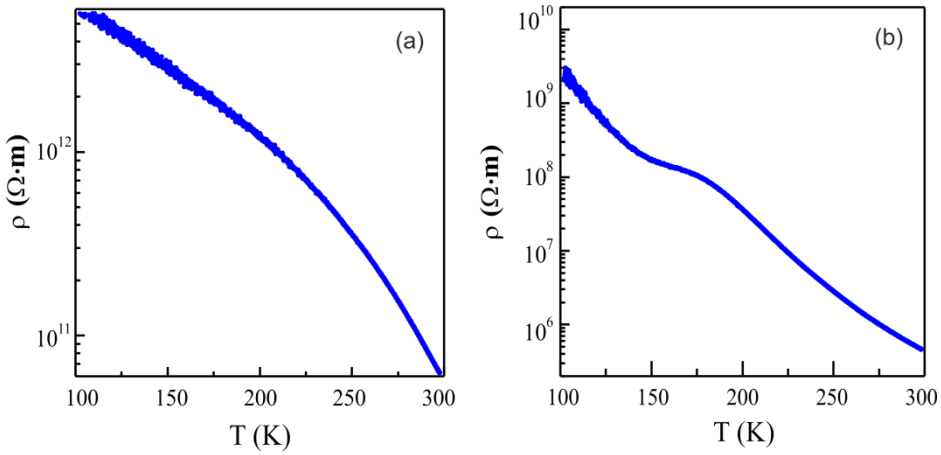


**Figure S7. Temperature dependence of resistivity of (a) $LaZrO_2N$ and (b) $NdHfO_2N$.**

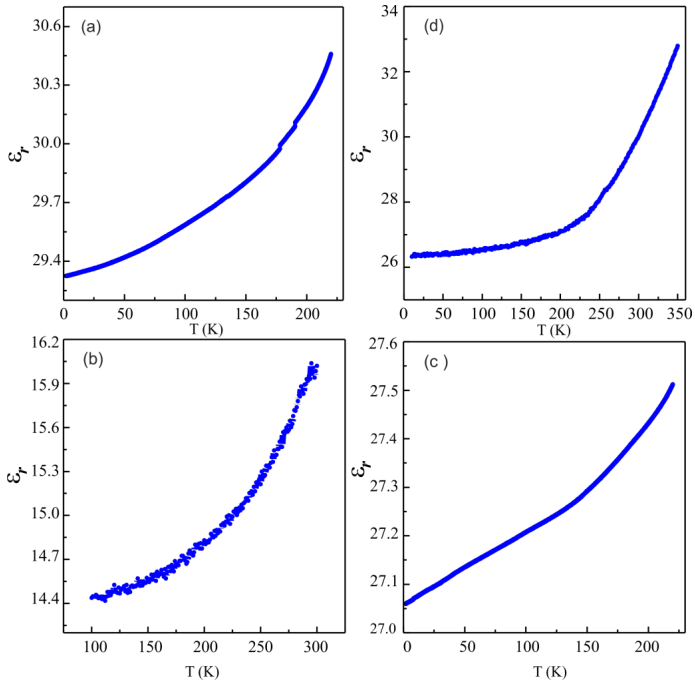


**Figure S8. Temperature dependence of dielectric permittivities of (a) $LaHfO_2N$, (b) $NdHfO_2N$, (c) $SmHfO_2N$ and (d) $LaZrO_2N$ measured at 100 kHz.**

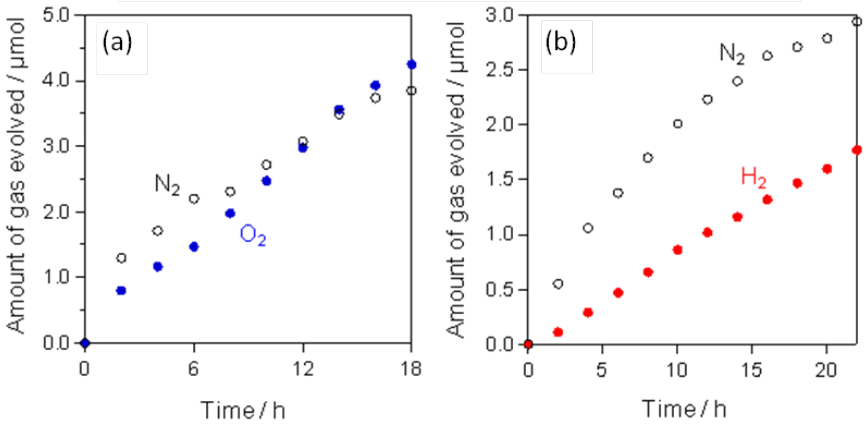


**Figure S9. $O_2$ evolution (blue spots) from 50 mg of $IrO_x$(1wt%)-$SmHfO_2N$ in 250 ml of a 10 mM solution of $AgNO_3$. $H_2$ evolution (red spots) from 50 mg of Pt(1wt%)-$SmHfO_2N$ in 250 ml of a 20 vol.% methanol solution and $N_2$ coevolution (black spots) under 300 W Xe lamp (λ > 300 nm).**

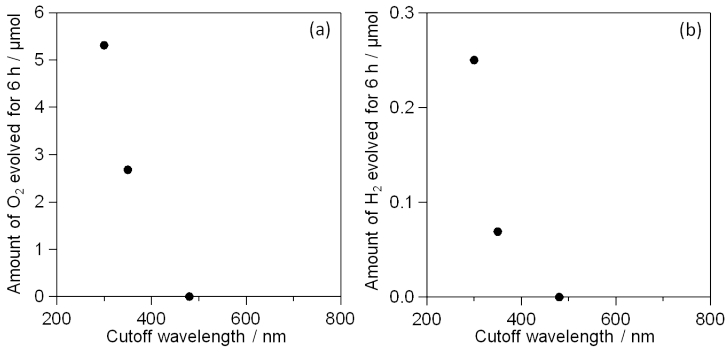


**Figure S10. Wavelength dependence of (a) $O_2$ evolution from 50 mg of $IrO_x$(1wt%)-$LaHfO_2N$ in 250 ml of a 10 mM solution of $AgNO_3$, and (b) $H_2$ evolution from 50 mg of Pt(1wt%)-$LaHfO_2N$ in 250 ml of a 20 vol.% methanol solution under 300 W Xe lamp with different cut-off filters (λ > 300, 350, 480 nm).**

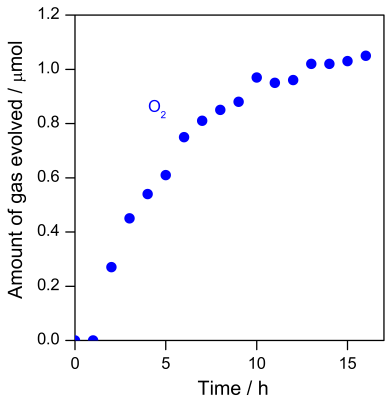


**Fig. S11. Time courses of $O_2$ evolution from aqueous methanol solution (20 vol%, 250 mL) or aqueous $AgNO_3$ solution (10 mM, 250 mL), respectively on unmodified $LaHfO_2N$.**

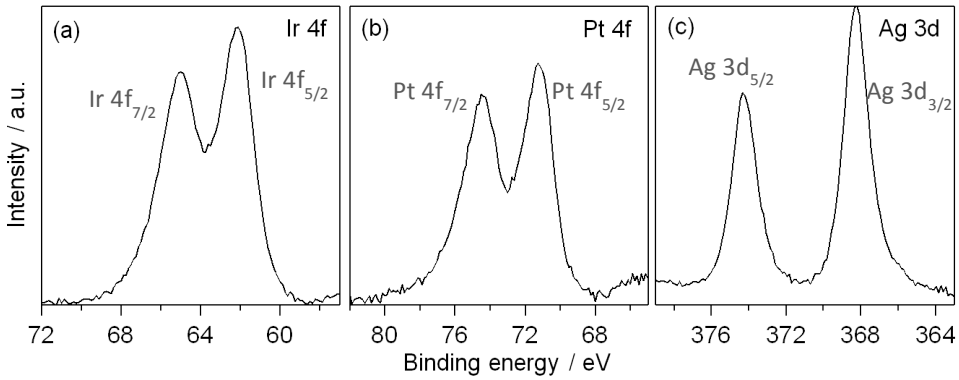


**Figure S12. X-ray photoelectron spectra of, (a) $IrO_x$-$LaHfO_2N$, (b) Pt-$LaHfO_2N$ and (c) $IrO_x$-$LaHfO_2N$ after $O_2$ evolution.**

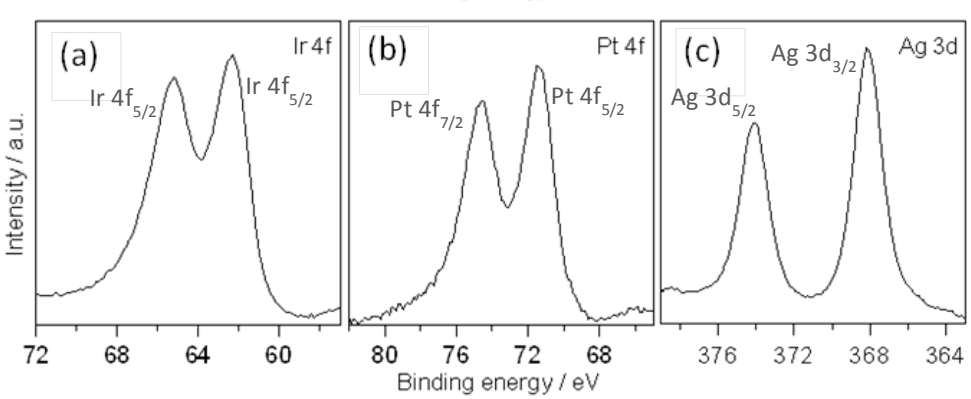


**Figure S13. X-ray photoelectron spectra of, (a) $IrO_x$-$SmHfO_2N$, (b) Pt-$SmHfO_2N$ and (c) $IrO_x$-$SmHfO_2N$ after $O_2$ evolution.**

[1] F. Fauth, I. Peral, C. Popescu, C. and M. Knapp, M. *Powder Diffraction* **28**, S360–S370 (2013).

[2] J.Rodríguez-Carvajal, *Phys. B*, 1993, **192**, 55.